A Journal of the Gesellschaft Deutscher Chemiker

Angewandte International Edition GDCh Chemie

www.angewandte.org

Accepted Article

Title: Three-Pronged Attack by Homologous Far-Red/NIR AIEgens to Achieve "1+1+1>3" Synergistic Enhanced Photodynamic Therapy

Authors: Wenhan Xu, Michelle M. S. Lee, Jing-Jun Nie, Zhihan Zhang, Ryan T. K. Kwok, Jacky W. Y. Lam, Fu-Jian Xu, Dong Wang, and Ben Zhong Tang

To be cited as: *Angew. Chem. Int. Ed.* 10.1002/anie.202000740
Angew. Chem. 10.1002/ange.202000740

Link to VoR: http://dx.doi.org/10.1002/anie.202000740
http://dx.doi.org/10.1002/ange.202000740

WILEY-VCH

10.1002/anie.202000740

WILEY-VCH

Three-Pronged Attack by Homologous Far-red/NIR AIEgens to Achieve "1+1+1>3" Synergistic Enhanced Photodynamic Therapy

Wenhan Xu,[a,e,+] Michelle M. S. Lee,[a,+] Jing-Jun Nie,[c] Zhihan Zhang,[a] Ryan T. K. Kwok,[a,d] Jacky W. Y. Lam,[a,d] Fu-Jian Xu,[c] Dong Wang,*[b] and Ben Zhong Tang*[a,d,e]

[a] W. Xu, M. M. S. Lee, Z. Zhang, Dr. R. T. K. Kwok, Dr. J. W. Y. Lam, Professor B. Z. Tang
Department of Chemistry, Hong Kong Branch of Chinese National Engineering Research Center for Tissue Restoration and Reconstruction, State Key Laboratory of Neuroscience, Department of Chemical and Biological Engineering, and Division of Life Science, The Hong Kong University of Science and Technology, Clear Water Bay, Kowloon, 999077, Hong Kong, China
E-mail: tangbenz@ust.hk
[b] Dr. D. Wang
Center for AIE Research, College of Materials Science and Engineering, Shenzhen University, Shenzhen, 518060, China
Email: wangd@szu.edu.cn
[c] Dr. J. -J. Nie, Dr. F. -J. Xu
Beijing Advanced Innovation Center for Soft Matter Science and Engineering, Beijing University of Chemical Technology, Beijing, 100029, China
[d] Professor B. Z. Tang
Center for Aggregation-Induced Emission, SCUT-HKUST Joint Research Institute, State Key Laboratory of Luminescent Materials and Devices, South China University of Technology, Guangzhou, 510640, China
[e] W. Xu, Professor B. Z. Tang
HKUST Shenzhen Research Institute, Shenzhen, China.
[+] These authors contributed equally to this work.

Supporting information for this article is given via a link at the end of the document.

Abstract: Photodynamic therapy (PDT) has long been proven to be a powerful therapeutic modality for cancer. However, PDT strategy is undiversified and stereotyped in recent years. Exploration of distinctive PDT protocol is highly in demand but remains a severe challenge. Herein, an unprecedented "1+1+1>3" synergistic strategy is proposed and validated for the first time. Three homologous luminogens with aggregation-induced emission (AIE) characteristics are rationally designed based on a simple backbone. By slight structural tuning, these far-red/near-infrared AIE luminogens are capable of specifically anchoring to mitochondria, cellular membrane and lysosome, and effectively generating reactive oxygen species (ROS). Notably, biological studies demonstrate that by combined usage of three AIE photosensitizers, multiple ROS sources synchronously derived from several organelles exhibit superior therapeutic effect than that of single organelle under the same photosensitizers' concentration. This strategy is conceptually and operationally simple, providing an innovative approach and renewed awareness of improving therapeutic effect through three-pronged PDT.

Introduction

Cancer, as a leading cause of death worldwide, has aroused great attention due to its limited early detection, rapid malignant progression, and late-stage metastasis.[1] In recent years, photodynamic therapy (PDT) has been discovered to induce apoptotic response of malignant cells through generation of radicals or reactive oxygen species (ROS) upon light irradiation. Since the first characterization of the photosensitizer Haematoporphyrin Derivative (HpD) in 1960,[2] PDT has been extensively explored to mediate tumor destruction.[3] Compared with surgery, radiotherapy and chemotherapy, PDT is highly repeatable, of lower costs, less invasive, and rarely has long term side effects. So far, PDT has been highly recognized in clinical practice, appearing as a promising alternative therapeutic protocol for various types of cancers.[4]

Numerous photosensitizers have been developed thereby for clinical trials. However, conventional photosensitizers often possess certain drawbacks, such as poor photostability and chemical stability, low fluorescence quantum yield in aqueous media, small Stokes shift, and limited ROS generation ability.[5] Moreover, some photosensitizers with extended π conjugation tend to be intrinsically planar in structure. This structural feature endows them with efficient luminescence in dilute solution but suppressed emission in aggregation state, which is commonly known as aggregation-caused quenching (ACQ).[6] ACQ characteristics often hamper the practical applications of fluorescent photosensitizers, especially for fluorescence image-guided photodynamic therapy, which has become one of the prominent modalities of cancer theranostics.[7] In this context, the emergence of photosensitizers with aggregation-induced emission (AIE) characteristics has triggered state-of-the-art development of cancer treatment. AIE luminogens (AIEgens) exhibit enhanced emission in aggregation state due to the principle of restriction of intramolecular motions (RIMs) that can block the nonradiative pathway upon aggregates formation.[8] In addition, AIE photosensitizers also show boosted ROS generation efficiency in aggregation state through promoting intersystem crossing rate.[9] Generally, an AIE photosensitizer is introduced inside cell to specifically target a type of subcellular organelle, and produce cytotoxic ROS upon light exposure to destroy the subcellular functions.[10] Some subcellular organelles including mitochondria, cellular membrane and lysosome, are wonderful cellular targeting sites for implementing PDT,[11] because these subcellular organelles are closely related to various cellular processes and playing indispensable roles in manipulating cellular status.

Notwithstanding the great significance, PDT strategy is stereotyped in recent years. Scientists have spent too much efforts on developing novel photosensitizers, whereas PDT

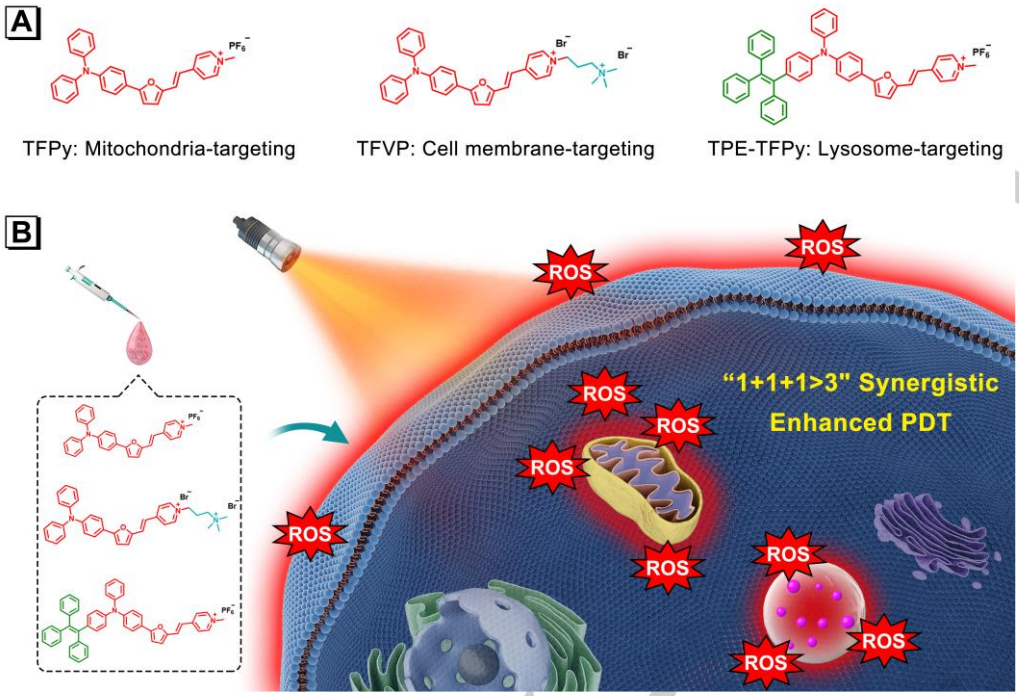

Figure 1. (A) Chemical structures of three AIEgens: TFPy, TFVP and TPE-TFPy. (B) Schematic illustration of using three AIEgens for achieving "1+1+1>3" synergistic enhanced photodynamic therapy.

itself as a distinct strategy has been paid little attention and remains barely exploited. As we know that the issues of inefficient therapy and drug resistance could be elegantly addressed by drug synergism, where equivalent therapeutic effect can be obtained with much fewer drug dose.[12] Inspired by synergistic effect of drugs, we are wondering if similar approach can be applied on PDT.[13] That is to say, what if multiple AIEgens are introduced into different organelles of cancer cells simultaneously? Is it possible to get synergistically enhanced PDT performance with lower photosensitizers' concentration?

In this work, a novel strategy is put forward and explored. Three novel AIEgens with the same backbone were well-tailored and used to specifically light up mitochondria, cellular membrane and lysosome, respectively. As displayed by *in vitro* and *in vivo* PDT experiments, when ROS is generated from multiple areas inside cells, it can lead to more severe cell death and prohibit tumor growth to a larger extent under the same concentration of photosensitizers (Figure 1). This is the first report to compare PDT efficacy between one and multiple ROS sources, thus demonstrating a smart strategy to improve therapeutic effect through three-pronged PDT.

Results and Discussion

Figure 1a presents the molecular structures of three novel compounds (TFPy, TFVP, and TPE-TFPy) with typical electron-donating and -accepting (D-A) feature. Such strong D-A interaction could facilitate intramolecular charge transfer (ICT) and thus allow longer wavelength emission. Besides, TPA moiety, a propeller-shaped nonplanar structure, can freely rotate in solution state resulting in nonradiative relaxation, and extend the intermolecular distance between two parallel planes in aggregates to produce enhanced emission, making them potentially AIE-active. Pyridinium ions not only impose electronic effects, but are well known to have targeting function as well. Compared with TFPy, TPE-TFPy attaches an extra triphenylethylene segment at lipophilic part, leading to more hydrophobic nature. In the case of TFVP, linking a tail of quaternary ammonium salt to pyridine moiety produces an elongated hydrophilic fragment, which greatly reduces the permeation ability of TFVP through cellular

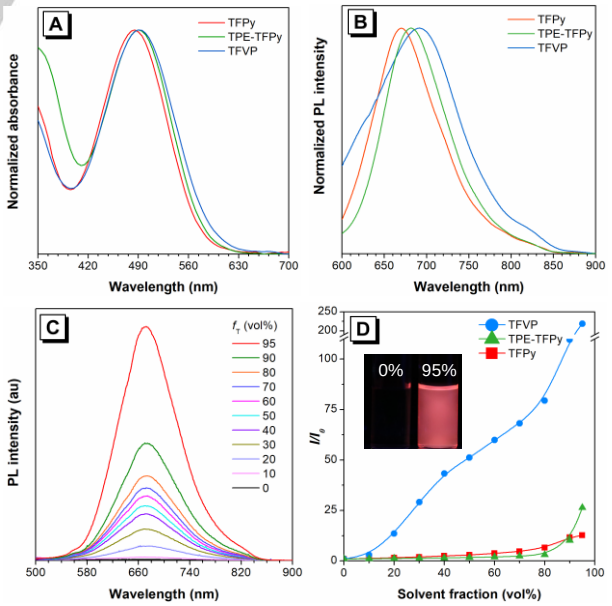

Figure 2. (A) Normalized absorption spectra of TFPy solution in DMSO, TPE-TFPy solution in DMSO and TFVP aqueous solution. (B) Normalized PL spectra of AIEgens in solid state. (C) PL spectra of TFVP (1×10^{-5} M) in H_2O/THF mixtures with different THF fractions (f_T); λ_{ex}: 480 nm. (D) Plots of relative PL intensity (I/I_0) versus the composition of different solution mixture of AIEgens. Inset: photos of H_2O and H_2O/THF mixture (f_T = 95%) of TFVP under 365 nm UV light.

Scheme 1. Synthetic route to TFPy, TPE-TFPy, and TFVP.

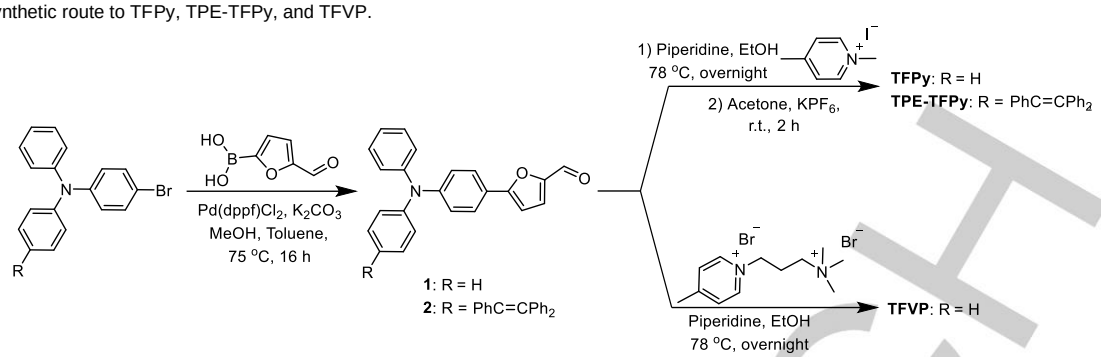

membrane.[14] It is believed that these three homologous compounds could possess different subcellular organelle-specific targeting behaviors. To verify these hypotheses, we started with the synthesis and characterization. As depicted in Scheme 1, the aldehyde intermediates **1** and **2** were obtained through Suzuki coupling reaction. The bromo-substituted TPA starting materials are either commercially available or accessible through reported procedures.[15] Knoevenagel condensation reaction between aldehyde and active methyl group was employed to produce target compounds TFPy, TFVP, and TPE-TFPy in moderate yields. Overall, the three AIEgens were facilely developed within a few reaction steps.

The photophysical properties of TFPy, TFVP and TPE-TFPy were characterized by UV-Vis and photoluminescence spectroscopies (Figure 2, Table S1). The three compounds possess similar absorption with maximum absorption peaks (λ_{abs}) at around 490 nm. Due to different solubility behavior, the AIE characteristics of TFPy and TPE-TFPy were investigated in DMSO/toluene mixture with different toluene fractions, whereas TFVP was measured in H_2O/THF mixture (Figure 2C, 2D and S2). Taking TFVP as an example, TFVP was barely emissive when fully dissolved in water. Upon increasing THF fraction, fluorescence emission intensity got boosted accordingly with a 218-time increment when THF fraction reached 95%. In case of TFPy and TPE-TFPy, the increment value is 12.6 and 26.4, respectively, demonstrating typical AIE characteristics of all three compounds. Notably, they exhibit far-red/near-infrared (FR/NIR) emission in solid state with relatively large stokes shifts (ca. 200 nm) (Figure 2B).

To better understand the optical properties of the AIEgens, density functional theory (DFT) calculations were carried out (Figure S1). The calculated natural transition orbitals (NTOs) show that all three molecules feature the “electron” delocalizing over TPA moiety and “holes” delocalizing at pyridine fragment, exhibiting strong charge transfer character. For all three AIEgens, the calculated decay energies of ca. 2 eV are relatively small, agreeing with their far red/NIR emission property. Singlet-triplet energy gaps (ΔE_{ST}) are determined to be around 1 eV due to sufficient separation of the corresponding NTOs, potentially making them promising PDT candidates by promoting ROS generation.

In vitro cellular imaging was carried out to evaluate their subcellular organelle targeting property using HeLa cell as model cell line. Thanks to the analogous maximum absorption of three AIEgens, fluorescence images can be acquired simultaneously using the same excitation at 488 nm. As illustrated in Figure 3, after respective incubations with TFPy, TFVP, and TPE-TFPy, reticulum-like mitochondria, ring-shaped cell membrane, and round or oval-shaped lysosome were clearly visualized showing bright fluorescence and high contrast to background signal. To further prove the targeting specificity, three commercial fluorescent probes, MitoTracker Green, CellMask Green, and LysoTracker Green, were employed to costain with AIEgens respectively. The costaining experiments showed perfect overlap as seen in the merged images with the Pearson’s correlation coefficients of over 90%, indicating the high targeting specificity, and validating that subtle structural alteration can lead to targetability variation. It was inferred that the mitochondria-staining behavior of TFPy could be attributed to its high efficiency of electrophoretic transmembrane migration, as well as appropriate binding ability between positively charged pyridinium moiety and the negatively charged interior of the transmembrane potential of mitochondria.[16] The low permeability coefficients resulted from the quite high free energy barrier of TFVP at membrane center could lead to its specific accumulation.[14] In the case of TPE-TFPy, it tends to form nano-sized aggregates in culture media due to the high hydrophobicity, and the in-situ generated aggregates can internalize into lysosome of HeLa cells through endocytosis and specifically light up lysosome upon photoexcitation. Therefore, when HeLa cells were cultured with these three AIEgens simultaneously, all of mitochondria, cell membrane and lysosome were highly emissive (Figure 3D).

Furthermore, photostability as an essential parameter to evaluate a fluorescence imaging agent was carefully investigated. Photostability assessment was carried out by continuous irradiation and sequential scanning. After 40 times of scan, minimal intensity loss was found for TPE-TFPy, TFPy and TFVP, whereas three fluorescent commercial probes especially LysoTracker Green suffered obvious fluorescence intensity decrease, demonstrating high photobleaching resistance of AIEgens (Figure 3E). With HeLa cell imaging and photostability data in hand, additional cellular uptake experiment using 4T1 cell line was performed as preliminary study for *in vivo* experiment. Similar bioimaging results were obtained, that is, TFPy, TFVP and TPE-TFPy exhibited strong affinity towards mitochondria, cellular membrane, and lysosome, respectively. The AIEgens exhibit high targeting specificity which was confirmed by superb costaining outcome with commercial probes (Figure 4A). Again, with three AIEgens staining jointly, the mitochondria, cellular membrane, and lysosome were well located and lighted up concurrently (Figure 4B).

In general, each organelle has its own specific function to manage cellular behavior. Briefly, mitochondria is a “power house” that can produce ATP to regulate cellular

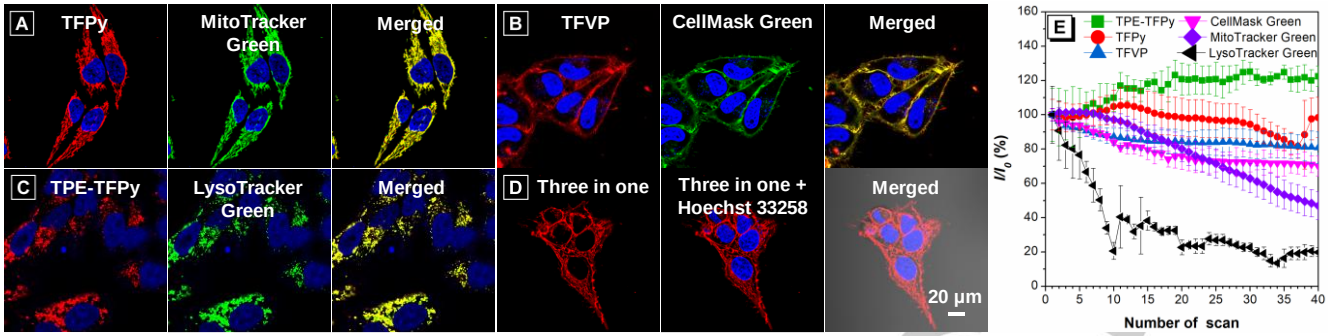

Figure 3. Co-localization test and photostability of TFPy, TFVP and TPE-TFPy. Confocal microscopic images of HeLa cells stained with A) TFPy (200 nM), MitoTracker Green (50 nM), and their merged images; B) TFVP (500 nM), CellMask Green (500 nM), and their merged images; C) TPE-TFPy (2 μM), LysoTracker Green (50 nM), and their merged images; D) three AIEgens (TFPy, TFVP and TPE-TFPy) altogether, three AIEgens and Hoechst 33258 (5 μM), and their merged images. E) Loss in fluorescence of HeLa cells stained with TFPy, TFVP, TPE-TFPy, MitoTracker Green, CellMask Green and LysoTracker Green with the number of scans of laser irradiation. Scanning rate: 22.4 s per frame. Scale bar = 20 μm.

metabolism.[17] Plasma membrane has selective permeability that protect the interior of cell from environment.[18] Lysosome's acidic interior can degrade obsolete biomolecules by various enzymes.[19] All the aforementioned three organelles are of vital importance to cellular status, therefore applying PDT to these regions can effectively induce cancer cell ablation. We are thereby prompted to examine PDT efficacy of three AIEgens, and more importantly, to explore whether PDT effectiveness will be boosted if three AIEgens are introduced concurrently.

Preliminary study was conducted by evaluating capability of ROS generation of three AIEgens, where 9,10-Anthracenediyl-bis-(methylene)-dimalonic acid (ABDA) was utilized as an indicator. Upon white light irradiation (4.2 mW·cm^{-2}), absorption peak of ABDA at 378 nm gradually decreased along with irradiation time in the presence of photosensitizers, while no obvious change was found for control group (Figure 5A and S3). Ce6 and Rose Bangel (RB), two well-known commercially available standard photosensitizers, were engaged as comparison. Both TFPy and TFVP exhibiting similar ROS generation efficacy performed better than Ce6, but not as efficient as RB. In addition, a sharp decline of absorbance intensity was found for TPE-TFPy, suggesting the superior ROS generation performance and great potential for PDT application. Besides, the ROS generation of "three in one" group suits well with linear combination of each individual AIEgen, suggesting that ROS generation of AIEgen is independent of each other (Figure S3). The singlet oxygen quantum yield was calculated using RB as a relative standard (Figure S4).

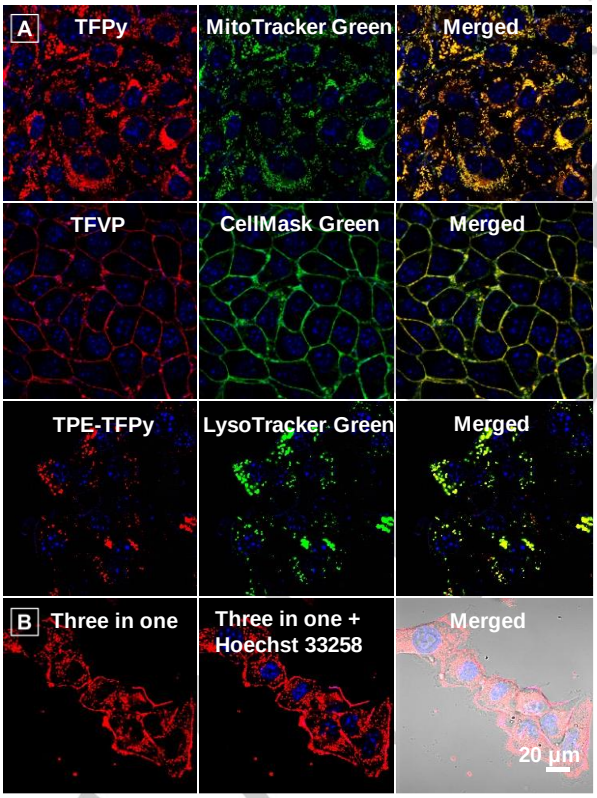

Figure 4. Co-localization test of AIEgens. Confocal microscopic images of 4T1 cells stained with A) TFPy (1 μM), MitoTracker Green (500 nM), and their merged images; TFVP (5 μM), CellMask Green (500 nM), and their merged images; TPE-TFPy (2 μM), LysoTracker Green (500 nM), and their merged images; B) three AIEgens (TFPy, TFVP and TPE-TFPy) altogether, three AIEgens and Hoechst 33258, and their merged images with bright field. Scale bar = 20 μm

Cytotoxicity of photosensitizer is a non-negligible factor to take into consideration. Desired photosensitizer should exhibit minimal cytotoxicity under dark condition, but produce efficient ROS to induce cell death upon light irradiation. Consequently, quantitative evaluation of PDT effect was applied on both HeLa Cell and 4T1 cell line through standard methylthiazolyldiphenyltetrazolium bromide (MTT) assay. Each AIEgen and an experimental group named "three in one" were evaluated. The "three in one" group was comprised of one third concentration of each AIEgen (1/3 TFPy, 1/3 TFVP, and 1/3 TPE-TFPy) to assure the overall concentration as same as other experimental groups. As illustrated in Figure 5B and 5D, after incubation for 24 h, negligible cellular viability reduction was found for HeLa cell with the concentration as high as 2.5 μM. In the case of 4T1 cell, the viability maintained 100 % at 5 μM, suggesting little dark toxicity of these AIEgens towards both cell lines. However, upon 20 min light irradiation, HeLa cell suffered severe viability loss with only 10 % remaining when the "three in one" group was at 2.5 μM (Figure 5C). Meanwhile, each individual AIEgen only exhibited moderate PDT efficacy. As for 4T1 cell, cell viability of "three in one" group started to decline at 2.5 μM, and almost complete cell death was induced at 5 μM (Figure 5E). Nevertheless, the individual AIEgen hardly displayed any therapeutic effect at 2.5 μM, and more than 60% cell viability still remained at 5 μM. Interestingly, ROS generation degree of "three in one" group was not as much as TPE-TFPy, but it caused more cell death. Both intracellular

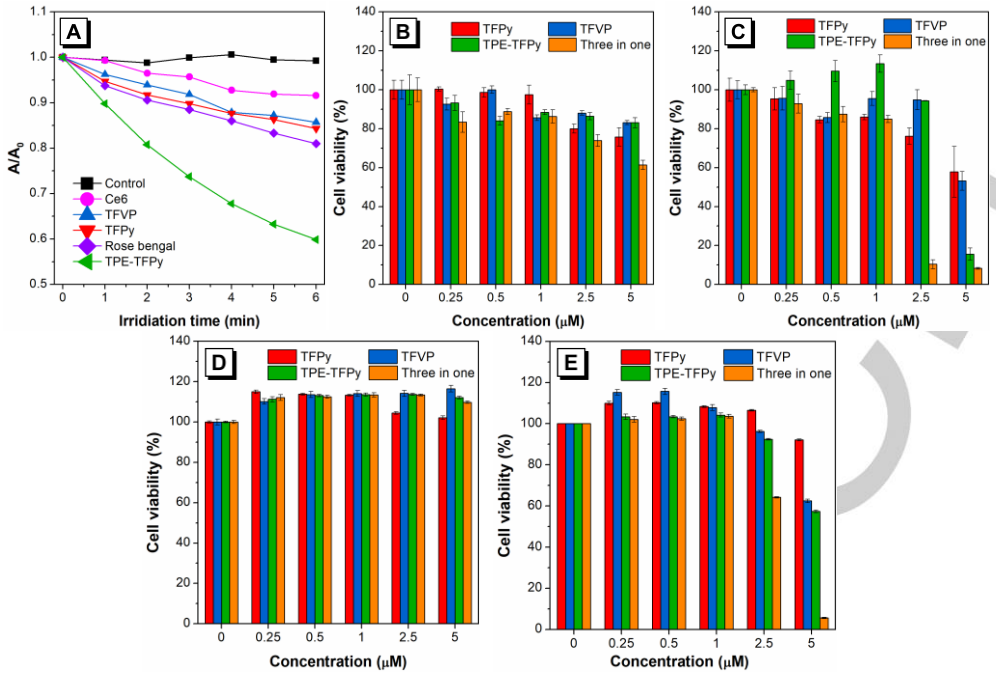

Figure 5. A) Normalized absorbance intensity of ABDA at 380 nm after photodecomposition by ROS upon white light irradiation. Cell viability of HeLa cell stained with different concentrations of AIEgens in the B) absence and C) presence of white light irradiation. Cell viability of 4T1 cell stained with different concentrations of AIEgens in the D) absence and E) presence of white light irradiation. IC50 values of "three in one" for HeLa and 4T1 cell are 2.72 and 1.40 μmol/L, respectively.

ROS generation detection by DCFH-DA and live/dead staining experiment assessed by FDA/PI supported the strong PDT effect of three in one group (Figures S5 and S6).The above results not only quantitatively demonstrated ROS generation ability and *in vitro* PDT effect of three AIEgens, but provided strong evidence that three-pronged PDT deriving out of multiple organelles can induce enhanced therapeutic effect as well.

Aiming to figure out whether combination enhanced PDT can be applied above cellular level, *in vivo* therapy experiment was conducted based on 4T1 breast tumor model. Tumor-bearing mice were divided into five groups, with one control group injecting PBS alone and four experimental groups (namely TFPy, TFVP, TPE-TFPy, and "three in one") injecting photosensitizers' aqueous solution (10^{-4} M, 100 μL). As depicted in Figure S7, after intratumor injection, intense fluorescence signals were captured at the tumor site in each case. At 24 h post-injection, tumor fluorescence was still visualized, indicating the remarkable tumor retention property of these AIEgens. Notably, when TFPy was injected individually, the accumulation in brain was detected by fluorescence signal. In "three in one" group, such fluorescence signal in brain region was insignificant, indicating TFPy may be trapped by other two AIEgens in the mixture. In the following study, tumor sites were exposed to white light irradiation for 10 min. As the treatment proceeded, tumor sizes were measured and evaluated every three days. It was found that all the four experimental groups were able to inhibit cancer cell proliferation in comparison with control group. It is worthy to note that the "three in one" group again manifested stronger hindrance of tumor growth than each photosensitizer alone, making combination enhanced PDT a convincing strategy to improve anti-tumor efficacy (Figure 6A). Moreover, body weight was monitored for each group to assess the toxicity. As shown in Figure 6B, no obvious body weight loss or difference was observed among different groups, owing to minimal toxicity of PDT approach. After 15 days of treatment, mice were sacrificed and major organs were sliced for histological hematoxylin and eosin (H&E) staining. All the tissue sections including heart, kidney, liver, lung, and spleen were evaluated, where no pathological change was observed (Figure S8). The body weight and H&E result above thus indicate that the photosensitizers, either individual or combined, were highly biocompatible.

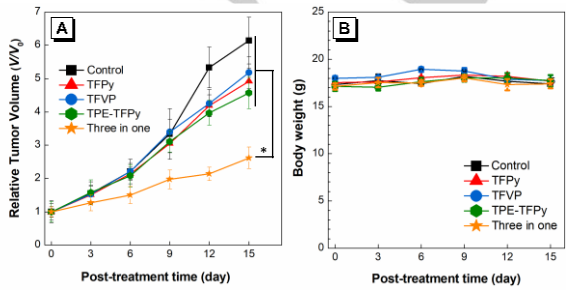

Figure 6. A) Tumor growth curves and B) body weight changes of mice in different treatment groups. * represents P < 0.05, in comparison between three in one group and other treatment groups.

Conclusion

To sum up, three homologous AIEgens with the same backbone were elaborately designed and facilely synthesized to specifically target three crucial subcellular organelles, mitochondria, cellular membrane and lysosome. All the AIEgens exhibited strong emission in far-red/NIR region, and preformed well in ROS generation. Both *in vitro* and *in vivo* PDT evaluations demonstrated that the treatment by three AIEgens together was capable of producing far superior therapeutic effect to each single AIEgen under the same total concentration due to the three-pronged attack towards cancer

cells, clearly suggesting "1+1+1>3" synergistic photodynamic therapy. To the best of our knowledge, the distinctive therapeutic protocol represents the first report of three-pronged PDT by concurrently working on multiple subcellular organelles. This study thus provides useful insights into achieving the variation of organelle targetability by subtle structural alteration, and offers an unprecedented strategy to inspire scientists to reconsider PDT from a different angle and study the mechanism behind.

Acknowledgements

This work was partially supported by the Natural Science Foundation of China (Grant No. 21801169), the Research Grants Council of Hong Kong (16305518 and C6009-17G), Science and Technology Plan of Shenzhen (JCYJ20160229205601482 and JCYJ20170818113538482), and the Innovation and Technology Commission (ITC-CNERC14SC01 and ITCRD/17-9). Animal experiments were approved by the China Committee for Research and Animals Ethics in compliance with the law on experimental animals.

Keywords: "1+1+1>3" Effect • Synergistic PDT• Aggregation-induced emission • Specific organelle-targeting

[1] F. Bray, J. Ferlay, I. Soerjomataram, R. L. Siegel, L. A. Torre, *A. Jemal, CA: Cancer J. Clin.* **2018**, 68, 394-424.
[2] R. L. Lipson, E. J. Baldes, *JAMA Dermatol.* **1960**, 82, 508-516.
[3] a) S. B. Brown, E. A. Brown, I. Walker, *Lancet* **2004**, 5, 497-508; b) L. Huang, Z. Li, Y. Zhao, Y. Zhang, S. Wu, J. Zhao, G. Han, *J. Am. Chem. Soc.* **2016**, 138, 14586−14591; c) L. Huang, Z. Li, Y. Zhao, J. Yang, Y. Yang, A. I. Pendharkar, Y. Zhang, S. Kelmar, L. Chen, W. Wu, J. Zhao, G. Han, *Adv. Mater.* **2017**, 29, 1604789.
[4] N. C. Zeitouni, A. R. Oseroff, S. Shieh, *Mol. Immunol.* **2003**, 39, 1133-1136; b) J. S. McCaughan, T. A. Nims, J. T. Guy, W. J. Hicks, T. E. Williams, L. R. Laufman, *JAMA Surg.* **1989**, 124, 74-80; c) J. Usuda, H. Kato, T. Okunaka, K. Furukawa, H. Tsutsui, K. Yamada, Y. Suga, H. Honda, Y. Nagatsuka, T. Ohira, *J. Thorac. Oncol.* **2006**, 1, 489-493; d) S. Yamaguchi, H. Tsuda, M. Takemori, S. Nakata, S. Nishimura, N. Kawamura, K. Hanioka, T. Inoue, R. Nishimura, *Oncology* **2005**, 69, 110-116; e) B. Shumaker, F. Hetzel, *Photochem. Photobiol.* **1987**, 46, 899-901; f) J. S. Mccaughan Jr, T. E. Williams Jr, B. H. Bethel, *Laser. Surg. Med.* **1986,** 6, 336-345; g) C. Frochot, S. Mordon, *J. Porphyr. Phthalocyanines* **2019**, 23, 347-357.
[5] S. K. Pushpan, S. Venkatraman, V. G. Anand, J. Sankar, D. Parmeswaran, S. Ganesan, T. K. Chandrashekar, *Anti-Cancer Agents Med. Chem.* **2002**, 2, 187-207.
[6] J. B. Birks, *Photophysics of Aromatic Molecules*, Vol. 704, Wiley, New York, **1970**.
[7] S. Singh, A. Aggarwal, N. V. S. D. K. Bhupathiraju, G. Arianna, K. Tiwari, C. M. Drain, *Chem. Rev.* **2015**, 115, 10261-10306.
[8] a) J. Mei, N. L. Leung, R. T. Kwok, J. W. Lam, B. Z. Tang, *Chem. Rev.* **2015**, 115, 11718-11940; b) J. Luo, Z. Xie, J. W. Lam, L. Cheng, H. Chen, C. Qiu, H. S. Kwok, X. Zhan, Y. Liu, D. Zhu, B. Z. Tang, *Chem. Commun*. **2001**, 1740-1741.
[9] L. Yang, X. Wang, G. Zhang, X. Chen, G. Zhang, J. Jiang, *Nanoscale* **2016**, 8, 17422-17426.
[10] a) Y. Yuan, C.-J. Zhang, M. Gao, R. Zhang, B. Z. Tang, B. Liu, *Angew. Chem. Int. Ed*. **2015**, 54, 1780-1786; b) Z. Zheng, T. Zhang, H. Liu, Y. Chen, R. T. K. Kwok, C. Ma, P. Zhang, H. H. Y. Sung, I. D. Williams, J. W. Y. Lam, K. S. Wong, B. Z. Tang, *ACS Nano* **2018**, 12, 8145-8159; c) M. M. S. Lee, L. Zheng, B. Yu, W. Xu, R. T. K. Kwok, J. W. Y. Lam, F. Xu, D. Wang, B. Z. Tang, *Mater. Chem. Front.* **2019**, 3, 1454-1461; d) D. Wang, M. M. S. Lee, W. Xu, R. T. K. Kwok, J. W. Y. Lam, B. Z. Tang, *Theranostics* **2018**, 8, 4925-4956.
[11] a) D. Kessel, Y. Luo, *Cell Death Differ.* **1999**, 6, 28; b) H. Huang, B. Yu, P. Zhang, J. Huang, Y. Chen, G. Gasser, L. Ji, H. Chao, *Angew. Chem. Int. Ed.* **2015**, 54, 14049-14052; c) Y. Yang, Q. Zhao, W. Feng, F. Li, *Chem. Rev.* **2013**, 113, 192-270.
[12] R. J. Tallarida, *J. Pharmacol. Exp. Ther.* **2001**, 298, 865-872.
[13] L. Yang, S. Zhang, X. Ling, P. Shao, N. Jia, M. Bai, *Acta Biomater.* **2017**, 54, 271-280.
[14] X. Zheng, D. Wang, W. Xu, S. Cao, Q. Peng, B. Z. Tang, *Mater. Horiz.* **2019**, 6, 2016-2023.
[15] W. Qin, K. Li, G. Feng, M. Li, Z. Yang, B. Liu, B. Z. Tang, *Adv. Func. Mater.* **2014**, 24, 635-643.
[16] L. B. Chen, *Annu. Rev. Cell Dev. Biol.* **1988**, 4, 155-181.
[17] H. M. McBride, M. Neuspiel, S. Wasiak, *Curr. Biol.* **2006**, 16, R551-R560.
[18] A. A. Spector, M. A. Yorek, *J. Lipid Res.* **1985**, 26, 1015-1035.
[19] J. P. Luzio, P. R. Pryor, N. A. Bright, *Nat. Rev. Mol. Cell Biol.* **2007**, 8, 622.

10.1002/anie.202000740

Entry for the Table of Contents

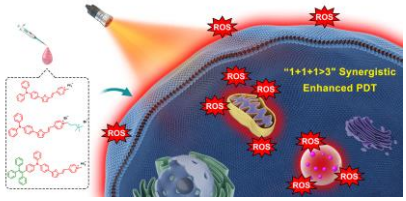

Three-pronged attack causes more damage: a synergistic enhanced photodynamic therapy (PDT) strategy is put forward for the first time by concurrently working on multiple subcellular organelles. Under the same photosensitizers' concentration, synchronous PDT treatment by three aggregation-induced emission luminogens (AIEgens) exhibits superior therapeutic effect than that of single AIEgen.